

Crystal Growth and Scintillation Properties of $\text{Cs}_2\text{NaGdBr}_6:\text{Ce}^{3+}$

Pin Yang, Xiaowang Zhou, Haoran Deng, Mark A. Rodriguez, Patrick L. Feng, Edgar V. D. van Loef, Kanai S. Shah, and F. Patrick Doty

Abstract—Single crystals of $\text{Cs}_2\text{NaGdBr}_6$ with different Ce^{3+} activator concentrations were grown by a two-zone Bridgman method. This new compound belongs to a large elpasolite halide (A_2BLnX_6) family. Many of these elpasolite compounds have shown high luminosity, good energy resolution and excellent proportionality in comparison to traditional scintillators such as CsI and NaI; therefore, they are particularly attractive for gamma-ray spectroscopy applications. This study investigated the scintillator properties of $\text{Cs}_2\text{NaGdBr}_6:\text{Ce}^{3+}$ crystals as a new material for radiation detection. Special focus has been placed on the effects of activator concentration (0 to 50 mol.%) on the photoluminescence responses. Results of structural refinement, photoluminescence, radioluminescence, lifetime and proportionality measurements for this new compound are reported.

Index Terms—Elasolite, halides, radioluminescence, scintillator photoluminescence.

I. INTRODUCTION

CERIUM activated rare-earth halides represent a new family of high performance inorganic scintillators with high luminosity, good energy resolution, and excellent proportionality in comparison to traditional scintillators such as CsI or NaI. These features are particularly attractive for advanced gamma-ray spectroscopy applications. Among many of these halide compounds, two groups of materials including tri-halides (LnX_3 ; Ln and X are the rare-earth and the halogen elements, respectively) [1], [2] and elpasolite halides (A_2BLnX_6 ; A, B are two different alkali elements) [3]–[5] have been actively pursued in the past decade. Some lithium based elpasolite halide compounds have also shown very promising results for gamma and thermal neutron detection. [6], [7] The distinctive performance exhibited by these new materials has accelerated

the research and development pace from basic material exploration to advanced device applications. In fact, in less than a decade single crystals of cerium doped LaBr_3 and $\text{Cs}_2\text{LiYCl}_6$ are under commercialization and are experiencing increasingly widespread use for radiation detection.

In this study, we investigated the photoluminescence and scintillation behavior of $\text{Cs}_2\text{NaGdBr}_6$ single crystals with and without cerium (Ce^{3+}) activator. This compound belongs to a large elpasolite halide family and initial radioluminescence responses were first reported by Rooh. [5] Because gadolinium compounds have less nonradiative interactions during the de-excitation, they are more suitable as host materials for Ce^{3+} activators as the trivalent gadolinium ion (Gd^{3+}) is one of the lanthanide ions that have few 4f energy levels with larger energy gaps between sublevels (Fig. 1, referred as the Dieke diagram). Hosts have many f-f transitions or small gaps between sublevels may cause strong optical absorption and nonradiative decay, as indicated by the color of these compounds. In addition, energy transfer from a higher $\text{Gd}^{3+}4f$ level to a lower $\text{Ce}^{3+}5d$ level is favorable (Fig. 1); therefore, the use of a gadolinium based host with Ce^{3+} activator can potentially increase their photoluminescence. Furthermore, the smaller ionic size and higher atomic number (Z) of Gd^{3+} will also increase its density and stopping power. These attractive features motivated our investigation into this new gadolinium containing elpasolite halide compound. The results of structural refinement, photoluminescence, radioluminescence, and decay time for the cerium activated $\text{Cs}_2\text{NaGdBr}_6$ (0 to 50 mol.%) are reported.

II. EXPERIMENTAL PROCEDURE

Single crystals of $\text{Cs}_2\text{NaGdBr}_6$ were grown by the Bridgman method, using stoichiometric amounts of CsBr, NaBr, and GdBr_3 . Nominal 2.5 mol.%, 5 mol.%, 7.5 mol.%, and 50 mol.% of CeBr_3 were added to substitute Gd^{3+} in the compound lattice as activator. These starting anhydrous compounds (>99.99%) were obtained from Sigma-Aldrich, which were mixed and loaded into fused quartz ampoules in an argon-filled glove box (humidity < 0.1 ppm). These ampoules were later vacuum sealed before crystal growth. Similar to other halides, this new compound is hygroscopic and all the measurements have to be performed either in dry environment or on encapsulated samples.

The structural refinements for undoped and Ce^{3+} doped $\text{Cs}_2\text{NaGdBr}_6$ were determined by x-ray powder diffraction using a specially designed Be dome sample holder [8] to avoid the exposure of the material to ambient air. Data were collected using a Siemens D500 diffractometer equipped with

Manuscript received June 20, 2012; revised September 21, 2012; accepted November 20, 2012. Date of current version April 10, 2013. This work is supported by the NNSA/DOE Office of Nonproliferation Research and Development, Proliferation Detection Program and Advanced Material Portfolio. Sandia National Laboratories is a multi-program laboratory managed and operated by Sandia Corporation, a wholly owned subsidiary of Lockheed Martin Corporation, for the U.S. Department of Energy's National Nuclear Security Administration under contract DE-AC04-94AL85000.

P. Yang and H. Deng, M. A. Rodriguez are with Sandia National Laboratories, Albuquerque, NM 87185-0958 USA (e-mail: pyang@sandia.gov).

F. P. Doty, P. L. Feng, and X. Zhou are with Sandia National Laboratories, Livermore, CA 94550 USA (e-mail: fpdoty@sandia.gov).

E. V. D. van Loef and K. S. Shah are with the Radiation Monitoring Devices Inc., Watertown, MA 02472 USA (e-mail: kshah@rmdinc.com).

Color versions of one or more of the figures in this paper are available online at <http://ieeexplore.ieee.org>.

Digital Object Identifier 10.1109/TNS.2013.2251473

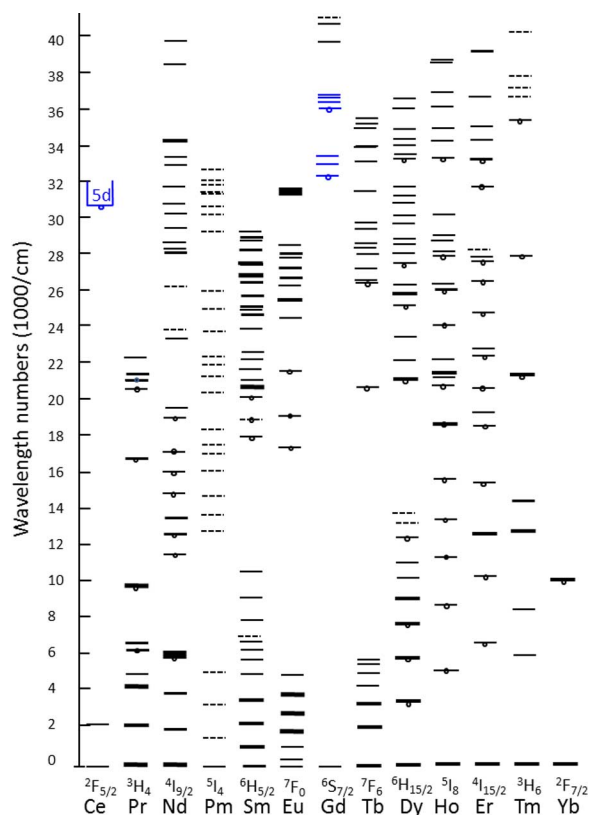


Fig. 1. Spectra and energy levels (f-f transitions) of lanthanide ions in inorganic crystals. Most of these ions, except cerium, gadolinium, and ytterbium, have many small energy gaps between sublevels and tend to produce nonradiative decay, therefore, not suitable for scintillator host. (Redrawn from G. H. Dieke, Interscience Publisher, New York, 1968).

a sealed tube x-ray source ($\text{Cu K}\alpha$) and a diffracted beam graphite monochromator. Fixed slits were employed for the measurement and generator settings were 40 kV and 30 mA. Typical scan parameters were $10\text{--}90^\circ$ 2θ with a step size of 0.04° and a various count times ranging from 1 to 20 seconds. Structure refinement of isolated phases was performed using GSAS software.

The photo-excitation and emission spectra of $\text{Cs}_2\text{NaGdBr}_6$ samples were measured by a standard fluorometer (PTI QuantaMaster, Birmingham, NJ), using a Xe arc lamp as light source which coupled with a double monochromator on the excitation side and a single monochromator on the emission side. The photo-excited quantum yield of these $\text{Cs}_2\text{NaGdBr}_6$ samples was measured, using the same excitation source with an integrating sphere [9] and a Teflon diffuser [10]. The radioluminescence spectra of $\text{Cs}_2\text{NaGdBr}_6$ were recorded using x-ray radiation from a Philips X-ray generator operated at 40 keV and 20 mA. The scintillation light was passed through a McPherson 0.2-m monochromator and detected with a cooled Burle C31034 photomultiplier tube (PMT) tube with a GaAs:Cs photocathode. The energy spectra and light output measurements were performed by coupling the crystals to a super bialkali R6233-100 PMT, operating at a voltage of -650 V. Pulse height spectra for the $\text{Cs}_2\text{NaGdBr}_6$ samples were recorded under 662 keV γ -ray excitation from a ^{137}Cs source. Scintillation decay time spectrum was measured under

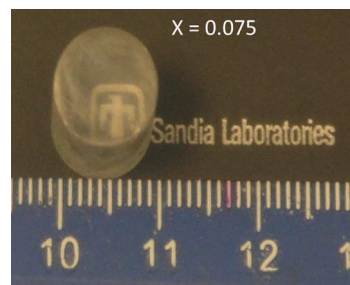


Fig. 2. 10 mm diameter $\text{Cs}_2\text{NaGd}_{0.925}\text{Ce}_{0.075}\text{Br}_6$ specimen (10 mm length) was cut and polished from a single crystal grown by the Bridgman method.

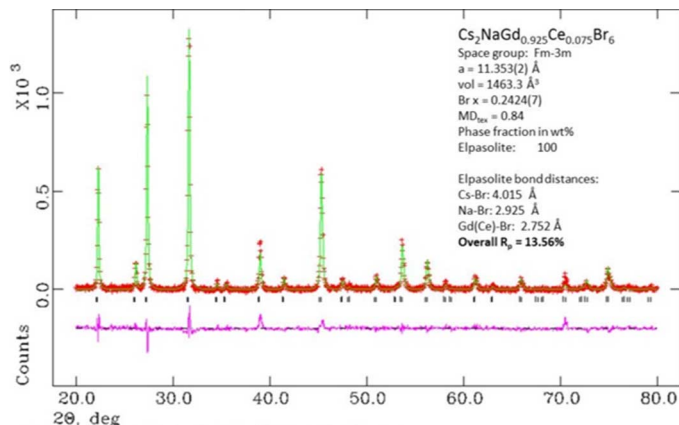


Fig. 3. X-ray diffraction pattern and structural refinement for $\text{Cs}_2\text{NaGd}_{0.925}\text{Ce}_{0.075}\text{Br}_6$.

2.5 MeV proton beam excitation, using the time-correlated single photon counting technique. [11] All these scintillation characterizations were measured at room temperature.

III. RESULTS AND DISCUSSION

A. Single Crystals and Structural Refinement

The cerium activated single crystals were grown in a fused quartz ampoule (10 mm diameter) by the Bridgman method. Cylinder shape of $\text{Cs}_2\text{NaGd}_{1-x}\text{Ce}_x\text{Br}_6$ (Fig. 2) crystals were cut with a wire saw and polished with 600, 800, and 1200 grit alumina sand papers in a dry room (humidity $< 0.2\%$) due to their hygroscopic nature.

Powder diffraction data obtained from crushed single crystals indicated that major peaks of these samples are consistent with the cubic elpasolite structure. However, a trace amount of NaBr and CsBr residual phases were occasionally detected in these samples. Fig. 3 shows a typical X-ray powder diffraction pattern and structural refinement results for these cerium activated $\text{Cs}_2\text{NaGdBr}_6$. Results indicated that $\text{Cs}_2\text{NaGdBr}_6$ (no Ce^{3+} doping) has a cubic structure (space group Fm3m (225)), with a lattice parameter of $11.348(1)$ Å and a calculated theoretical density of 4.207 g/cm³. When the Ce^{3+} activator concentration increases from 0 to 7.5 mol.%, the crystal symmetry does not change and the lattice parameter increases linearly from 11.348 Å to 11.366 Å, indicating a complete solid solution was formed within this composition range, as the larger Ce^{3+} cations substitute the smaller Gd^{3+} in the host lattice.

The potential of forming a cubic elpasolite halide has a strong advantage over the anisotropic tri-halide compounds when it comes to the crystal growth of practical sizes for detector applications. Many thermomechanical stress problems associated with the solidification process (e.g., anisotropic thermal expansion [12], and perfect cleavage on slip planes [13]) can be avoided, particularly for the growth of larger crystals. In addition, being an optical isotropic medium can significantly reduce the amount of light scattering at grain boundaries in comparison to birefringent materials such as these tri-halide compounds. Therefore, polycrystalline materials with high optical quality, low-cost can potentially be fabricated in large sizes which in turn will increase the widespread use of these high performance materials for radiation detection applications.

B. Optical Spectroscopy

The optical excitation (dotted line) and emission (solid line) spectra for $\text{Cs}_2\text{NaGdBr}_6$ are given in Fig. 4. Results indicate that this undoped compound behaves like an “intrinsic” scintillator i.e., emitting light under excitation without activator. The excitation spectrum shows a broad band between 320 nm to 380 nm. However, the source of this strong excitation, peaked at 350 nm, is not clear. The absence of 4f-4f transitions for Gd^{3+} in this range (Fig. 1) suggested that this band may be closely related to lattice defects in the crystal. Among all the possible lattice defects, bromine anion vacancies seem most likely to be the cause. Bromine becomes extremely volatile at high temperature which can result in dark, reduced bromide compounds. [14] The often observed small black particles floating on the melt or residing at the top section of single crystals in our experiment are indicative of these defects formation. It is well known that the formation of anion vacancies can introduce color centers [15] and distort the local symmetry [16] in the lattice, both of which can significantly increase the optical absorption. [15], [16] Pogatshnik [15] attributed the broadening of the 350 nm band to the ionization of color centers followed by trapping of these photoionized charge carriers for cubic gadolinium gallium garnets. This interpretation is consistent with the observation of small excitation peaks found at 274 nm and 313 nm. As indicated by energy levels of Gd^{3+} at $\sim 36,000 \text{ cm}^{-1}$ and $32,000 \text{ cm}^{-1}$ on the Dieke diagram (Fig. 1), these peaks correspond to the gadolinium ${}^6\text{I}_{7/2} - {}^8\text{S}_{7/2}$ and ${}^6\text{P}_{7/2} - {}^8\text{S}_{7/2}$ transitions. [17] Generally these excitations are forbidden since Gd^{3+} occupies a centrosymmetric octahedral site (O_h) in the elpasolite halide lattice. The local symmetry distorted by lattice defects will relax the constraint for 4f-4f transitions; therefore, it is not surprised to observe these weak transitions in the undoped compound.

A strong emission band is observed at 427 nm followed by a weak, broad band emission centered at 550 nm when the sample is excited at 350 nm. In addition, the excitation band of the 550 nm emission also peaks at 350 nm (not shown) which is consistent with the excitation spectrum reported for the gadolinium gallium garnet where lattice defects and color centers are known to exist. [15] Therefore, these bands must come from a same source. Based on the similarity found in the photoluminescence responses in $\text{Cs}_2\text{NaGdBr}_6$ and other two gadolinium based cubic compounds, [15] color centers associated with lattice defects are believed to be the primary source for these emissions.

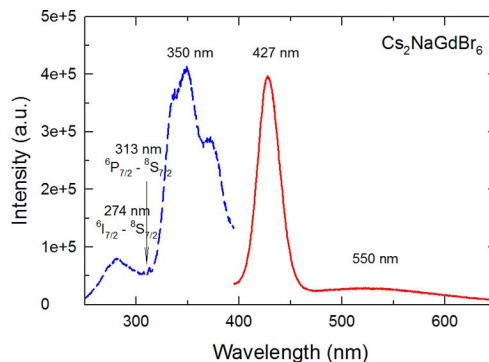


Fig. 4. The excitation and emission spectra for intrinsic $\text{Cs}_2\text{NaGdBr}_6$.

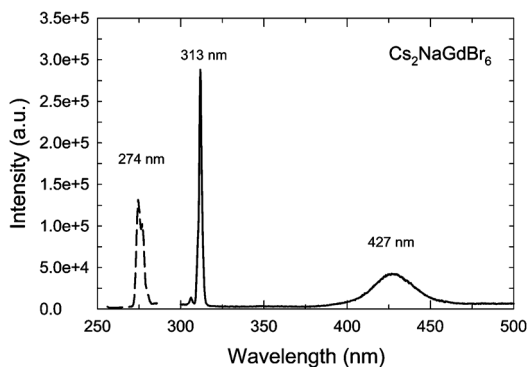


Fig. 5. The energy transfer of Gd^{3+} from 274 nm (${}^8\text{S}_{7/2} - {}^6\text{I}_{7/2}$, dotted line) to 313 nm (${}^6\text{P}_{7/2} - {}^8\text{S}_{7/2}$, solid line) and the color center luminescence at 427 nm.

Fig. 5 illustrates the energy transfer from gadolinium ${}^8\text{S}_{7/2}$ to ${}^6\text{I}_{7/2}$ excitation (274 nm, excitation, dotted line) to a longer wavelength 4f-4f emission at 313 nm (${}^6\text{P}_{7/2} - {}^8\text{S}_{7/2}$, emission, solid line) and the color center luminescence at 427 nm. [15] An additional weak emission band near 624 nm, corresponding to the $\text{Gd}^{3+} {}^6\text{G}_{7/2} - {}^6\text{P}_j$ transition, [17] is also observed (not shown). These observations immediately suggest that both color centers and Gd^{3+} 4f-4f transitions play an important role in scintillation for this “intrinsic” scintillator.

Fig. 6 shows excitation and emission spectra measured for cerium doped $\text{Cs}_2\text{NaGd}_{1-x}\text{Ce}_x\text{Br}_6$ samples. The excitation spectra shown on Fig. 6(a) exhibit a broad excitation band from 325 nm to 380 nm, and this band widens as cerium concentration increases. The emission spectra (Fig. 6(b)) for these samples show two broad bands peaked around 382 nm and 420 nm. This doubled peaked emission pattern can be assigned to the 5d-to-4f cerium transitions from the lowest 5d excited state to the two spin-orbit split ${}^2\text{F}_{5/2}$ and ${}^2\text{F}_{7/2}$ ground state levels. The reason for the systematic decrease in the relative intensities of the shorter wavelength emission (i.e., 382 nm) with the increase of Ce^{3+} concentration is still not clear. However, such behavior seems to be commonly to many elpasolite halides [3]–[5], [18] and may deserve for a detailed study.

Since Ce^{3+} is an effective activator, weak color center emission detected in the “intrinsic” $\text{Cs}_2\text{NaGdBr}_6$ (Fig. 4.) was almost completely inundated by the 5d-to-4f Ce^{3+} transitions.

Optical quantum yield plays an important role in the de-excitation processes as it governs the efficiency of light output

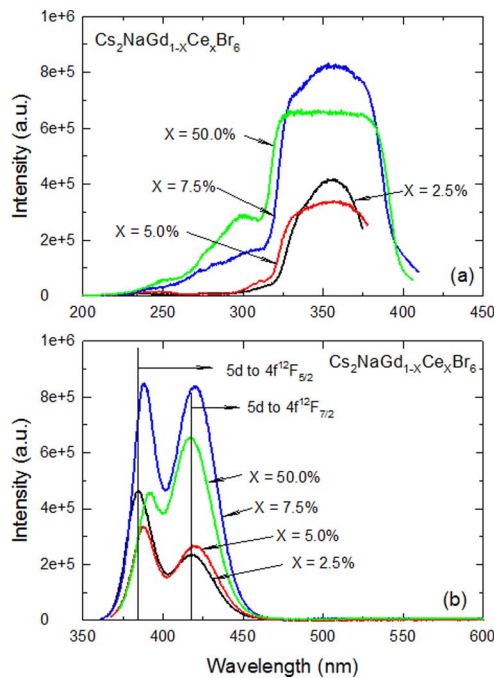


Fig. 6. Optical excitation (a) and emission (b) spectra of $\text{Cs}_2\text{NaGd}_{1-x}\text{Ce}_x\text{Br}_6$ crystals. The excitation spectra were measured at 382 nm emission for 2.5% and 5.0% samples and 420 nm for 7.5% and 50.0% samples, while the emission spectra were collected under 351 nm excitation.

at the activator site and as such it is closely related to the luminosity of the scintillator. The quantum yield (QY) for the $\text{Cs}_2\text{NaGd}_{1-x}\text{Ce}_x\text{Br}_6$ solid solution was determined by a powder method. Prior these measurements, the accuracy of our system was confirmed by a 0.1 M quinine sulfate solution (QY = 58%). Fig. 7 depicts the change of optical QY for the $\text{Cs}_2\text{NaGd}_{1-x}\text{Ce}_x\text{Br}_6$ solid solution ($x = 0$ to 0.5). It is evident from this figure that Ce^{3+} is an effective activator, as the QY increases from 29.3%, 48.0%, 50.2%, to 67.4% as its concentration increase from 0%, 2.5%, 5.0%, to 7.5%. However, when the Ce^{3+} concentration increases to 50%, the QY drops back to 60.2%, suggesting a slight concentration quenching for the $\text{Cs}_2\text{NaGdBr}_6$ scintillator.

C. Radioluminescence

The radioluminescence emission of the undoped $\text{Cs}_2\text{NaGdBr}_6$ measured under x-ray excitation exhibits a spectrum similar to its photoluminescence spectrum (not shown), with a small $\text{Gd}^{3+}6\text{P}_{7/2} - 8\text{S}_{7/2}$ emission peak at 313 nm and a large emission peak at 427 nm, as well as a broad emission band centered at 550 nm. When 5% Ce was added, a double-peak emission becomes dominate due to 5d-to-4f transitions of Ce^{3+} (Fig. 8). The additional peak observed at 626 nm, same peak height of 313 nm peak, is an artifact due to a second-order grating effect from optics. Apparently, the amount of radioluminescence due to the f-f transition from Gd^{3+} is relative small in comparison to the 5d-to-4f transitions from Ce^{3+} .

Fig. 9 shows the energy spectra and light output measurements of the $\text{Cs}_2\text{NaGd}_{0.95}\text{Ce}_{0.05}\text{Br}_6$ crystal under 662 keV gamma rays irradiation from a ^{137}Cs source. The spectrum is

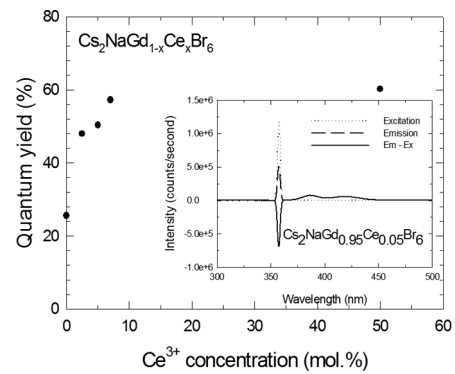


Fig. 7. The optical quantum yield as a function of Ce^{3+} activator in the $\text{Cs}_2\text{NaGd}_{1-x}\text{Ce}_x\text{Br}_6$ solid solution. Insert shows the quantum yield measurement for $\text{Cs}_2\text{NaGd}_{0.95}\text{Ce}_{0.05}\text{Br}_6$ crystal at 357 nm.

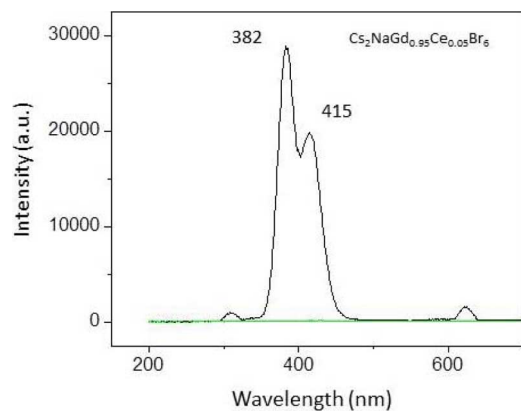


Fig. 8. Radioluminescence spectrum of $\text{Cs}_2\text{NaGd}_{0.95}\text{Ce}_{0.05}\text{Br}_6$ crystal. The green line on the plot represents the background response.

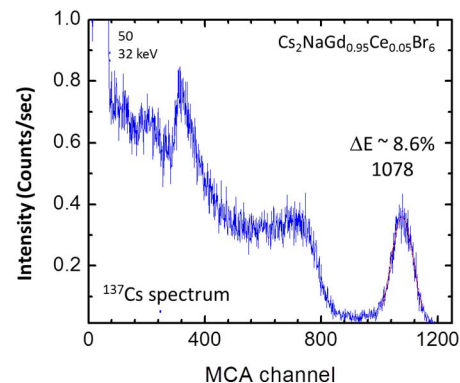


Fig. 9. Pulse height spectrum of $\text{Cs}_2\text{NaGd}_{0.95}\text{Ce}_{0.05}\text{Br}_6$ crystal under ^{137}Cs excitation.

recorded with a shaping time of 4 μs at room temperature. Energy resolution is obtained from FWHM of the photopeak using a single Gaussian function. Results show the energy resolution of this $\text{Cs}_2\text{NaGd}_{0.95}\text{Ce}_{0.05}\text{Br}_6$ sample at 662 keV is $\sim 8.6\%$, which is still far from the energy resolution of $\text{LaBr}_3:\text{Ce}^{3+}$ (4.2%), [19] but is comparable with that of NaI:Tl . Further improvement in the energy resolution could be achieved with better detector fabrication and assembly, and higher quality crystal growth.

The amount of light yield is estimated by a ratio method where radioluminescence spectra of the same size crystals

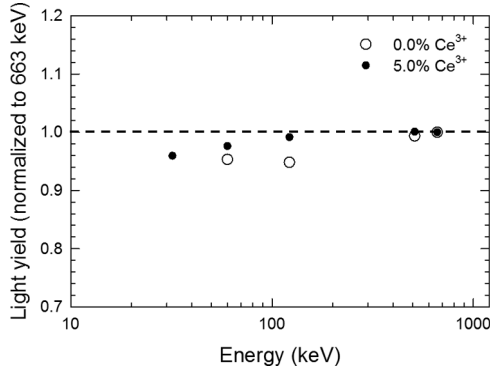


Fig. 10. The non-proportionality plots for $\text{Cs}_2\text{NaGdBr}_6$ and $\text{Cs}_2\text{NaGd}_{0.95}\text{Ce}_{0.05}\text{Br}_6$ crystals. Within the measured range the non-proportionality for $\text{Cs}_2\text{NaGdBr}_6$ (open) and $\text{Cs}_2\text{NaGd}_{0.95}\text{Ce}_{0.05}\text{Br}_6$ (close) is within 5% and 4%, respectively.

of $\text{Cs}_2\text{NaGd}_{0.925}\text{Ce}_{0.075}\text{Br}_6$ and NaI:Tl (Spectra Physics) are taken by a R1924 PMT (Hamamatsu) under the same gain and the same 1 microsecond shaping time with a ^{137}Cs source. Based on the quantum efficiency values of the PMT at the emission maxima of $\text{Cs}_2\text{NaGd}_{0.925}\text{Ce}_{0.075}\text{Br}_6$ ($\sim 24\%$, at 382 nm) and NaI:Tl ($\sim 22\%$, at 420 nm) and the relative intensity of photopeak for these crystals, light yield for $\text{Cs}_2\text{NaGd}_{0.925}\text{Ce}_{0.075}\text{Br}_6$ crystal is estimated to be $\sim 40,000$ photons/MeV, which is slightly higher than values reported by Rooh for a similar composition. [5] The amount of light yield for the investigated sample is lower than the best elpasolite data reported for $\text{Cs}_2\text{NaLaI}_6:\text{Ce}^{3+}$ ($\sim 46,000$ photons/MeV) [3] and is greater than other Ce^{3+} activated elpasolite crystals such as $\text{Cs}_2\text{LiLaCl}_6$ [20] and $\text{Cs}_2\text{LiYCl}_6$. [21], [22]

The non-proportionality of light output per energy unit versus energy of excitation measured for $\text{Cs}_2\text{NaGdBr}_6$ and $\text{Cs}_2\text{NaGd}_{0.95}\text{Ce}_{0.05}\text{Br}_6$ crystals is shown in Fig. 10. The non-proportionality is closely related to the energy resolution. Scintillators exhibiting non-proportional response will perform worse than expected energy resolution based on the photon statistics. Photopeaks of various gamma ray energies, including ^{137}Cs (32 keV, 662 keV), ^{22}Na (511, 1275 keV), ^{57}Co (122, keV) and ^{241}Am (60 keV), were used to construct the non-proportionality plot, which spans the energy range of 60–1275 keV. These values were then normalized to the incident energy and plotted relative to the ^{137}Cs 662 keV result. Results show the collected data deviate slightly from the straight line only at lower energies. Results show that the deviations from linearity for undoped and doped (5% Ce^{3+}) samples are less than 5% and 4%, respectively.

These values are comparable to cerium activated LaBr_3 and LaCl_3 which showed 4% and 7% non-proportionality in the similar energy range, [23] but are substantially better than that of many established scintillators such as LSO (35%), [24] NaI:Tl (20%) and CsI:Tl (20%). [25]

Energy resolution is particularly important for gamma-ray spectroscopy applications. Fig. 11 shows the energy resolution as a function of gamma-ray energy for undoped and 5% cerium doped $\text{Cs}_2\text{NaGdBr}_6$, collected from pulse height spectra of different radioactive isotopes. Apparently,

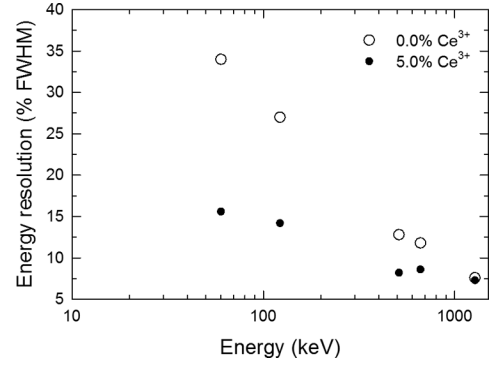


Fig. 11. Energy resolution as a function of gamma-ray energy for $\text{Cs}_2\text{NaGdBr}_6$ (open) and $\text{Cs}_2\text{NaGd}_{0.95}\text{Ce}_{0.05}\text{Br}_6$ (close) crystals.

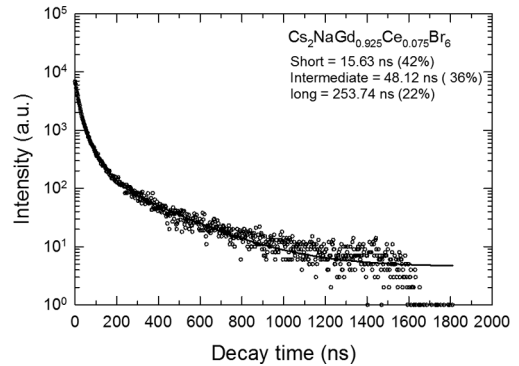


Fig. 12. Scintillation decay time spectrum for $\text{Cs}_2\text{NaGd}_{0.925}\text{Ce}_{0.075}\text{Br}_6$ crystal obtained by the proton beam excitation at 2.5 MeV. Solid line represents the fitting result.

$\text{Cs}_2\text{NaGdBr}_6:5\% \text{Ce}^{3+}$ has a much better energy resolution than the intrinsic $\text{Cs}_2\text{NaGdBr}_6$ scintillator. The difference in energy resolution can be attributed to the luminosity as indicated by their optical quantum yield (Fig. 7). However, the difference becomes progressively smaller as gamma energy increases, as expected from photon statistics.

The scintillation decay time spectrum of $\text{Cs}_2\text{NaGd}_{0.925}\text{Ce}_{0.075}\text{Br}_6$ crystal was measured under 2.5 MeV proton beam excitation, using a single photon counting technique (Fig. 12). The decay curve was fitted with the sum of three exponential decay time components. These decay time components and their relative contributions to the total light output are given in Fig. 12. The relative time scale for these components reflects the energy transfer mechanisms, which will be studies in the near future.

IV. SUMMARY

This study reported the initial investigation of $\text{Cs}_2\text{NaGdBr}_6$ scintillator as a function of cerium concentration. Results indicate that $\text{Cs}_2\text{NaGdBr}_6$ is an “intrinsic” scintillator. Its scintillation performance can be greatly enhanced by cerium activator. The cerium activated $\text{Cs}_2\text{NaGdBr}_6$ exhibits typical 5d-4f emissions in the 350 nm to 450 nm range, which is well matched with photomultiplier spectral sensitivity. The increase of cerium concentration in the host lattice does not change the cubic elpasolite structure, but greatly enhances the optical quantum yield, linearity response and energy resolution. These results indicate that

the cerium activated $\text{Cs}_2\text{NaGdBr}_6$ is well positioned to compete with traditional scintillators such as CsI and NaI in many applications. Further improvement in energy resolution is expected with improved detector fabrication and crystal quality.

REFERENCES

- [1] O. Guillot-Noel, J. T. M. de Hass, P. Dorenbos, C. W. E. van Eijk, K. Kramer, and H. U. Gudel, "Optical and scintillation properties of cerium-doped LaCl_3 , LuBr_3 and LuCl_3 ," *J. Lumin.*, vol. 85, pp. 21–35, 1999.
- [2] K. S. Shah, J. Globo, W. H. Higgins, E. V. D. van Loef, W. W. Moses, S. E. Derenzo, and M. J. Weber, "CeBr₃ scintillators for gamma-ray spectroscopy," *IEEE Trans. Nucl. Sci.*, vol. 52, no. 6, pp. 3157–3159, 2005.
- [3] J. Globo, E. V. D. van Loef, W. M. Higgins, and K. S. Shah, "Scintillation properties of $\text{Cs}_2\text{NaLaF}_6:\text{Ce}$," in *Proc. 2006 IEEE NSS Conf. Rec.*, 2006, pp. 1208–1211.
- [4] U. Shirwadkar, J. Globo, E. V. van Loef, R. Hawrami, S. Mukhopadhyay, A. Churilov, W. M. Higgins, and K. S. Shah, "Scintillation properties of $\text{Cs}_2\text{LiLaBr}_6$ (CLLB) crystals with varying Ce³⁺ concentration," in *Nucl. Instr. Meth. A.*, 2010, doi:10.1016/j.nima.2010.08.050.
- [5] G. Rooh, H. J. Kim, H. Park, and S. Kim, "Luminescence and scintillation characterization of $\text{Cs}_2\text{NaGdBr}_6:\text{Ce}^{3+}$ Single Crystal," *J. Lumin.*, vol. 132, pp. 713–716, 2012.
- [6] A. Bessiere, P. Dorenbos, C. W. E. van Eijk, K. W. Kramer, and H. U. Gudel, "Luminescence and scintillation properties of $\text{Cs}_2\text{LiYCl}_6:\text{Ce}^{3+}$ for γ and neutron detection," *Nucl. Instr. Meth. A.*, vol. 537, pp. 242–246, 2005.
- [7] D. W. Lee, L. C. Stonehill, A. Kimenko, J. R. Terry, and S. R. Tornga, "Pulse-shape analysis of $\text{Cs}_2\text{LiYCl}_6:\text{Ce}^{3+}$ scintillator for neutron and gamma-ray discrimination," *Nucl. Instr. Meth. A.*, vol. 664, pp. 1–5, 2012.
- [8] M. A. Rodriguez, T. J. Boyle, P. Yang, and D. L. Harris, "A beryllium dome specimen holder for XRD analysis of air sensitive materials," *Powder Diffraction*, vol. 23, pp. 121–124, 2008.
- [9] A. K. Gaigalas and L. Wang, "Measurement of the fluorescence quantum yield using a spectrometer with an integrating sphere detector," *Res. Natl. Inst. Stand. Technol.*, vol. 113, pp. 17–28, 2008.
- [10] L. S. Rohwer and J. E. Martin, "Measuring the absolute quantum efficiency of luminescent materials," *J. Lumin.*, vol. 115, pp. 77–90, 2005.
- [11] L. M. Bollinger and G. E. Thomas, "Measurement of the time dependence of scintillation intensity by a delayed-coincidence method," *Rev. Sci. Instrum.*, vol. 32, pp. 1044–1050, 1961.
- [12] F. P. Doty, D. McGregor, M. Harrison, K. Findley, and R. Polichar, "Basic materials studies of lanthanide halides scintillators," in *Proc. SPIE 6707*, 2007, pp. 670705–670705.
- [13] F. P. Doty, D. McGregor, M. Harrison, K. Findley, R. Polichar, and P. Yang, "Basic materials studies of lanthanide halides scintillators," in *Mater. Res. Soc. Symp. Proc.*, 2007, vol. 1038, pp. 1–7.
- [14] K. Kramer, T. Schleid, M. Schulze, W. Urland, G. Mayer, and Z. Anorg., "Three bromides of lanthanum: LaBr_2 , La_2Br_5 , and LaBr_3 ," *Allg. Chem.*, vol. 505, pp. 61–70, 1989.
- [15] G. J. Pogatschnik, L. S. Chen, Y. Chen, and B. D. Evans, "Optical properties of color centers in calcium-stabilized gadolinium gallium garnets," *Phys. Rev. B*, vol. 43, no. 2, pp. 1787–1794, 1991.
- [16] W. L. Warren, K. Vanheusden, C. H. Seager, D. R. Tallant, J. A. Tuchman, S. D. Silliman, and D. T. Brower, "Local Ce environments and their effects on optical properties of SrS phosphors," *J. Appl. Phys.*, vol. 80, no. 12, pp. 7036–7040, 1996.
- [17] A. J. de Vries and G. Blasse, "Two-photon transitions of Gd^{3+} in cubic $\text{Cs}_2\text{NaGdCl}_6$," *J. Chem. Phys.*, vol. 88, pp. 7312–7316, 1988.
- [18] G. Rooh, H. Kang, H. J. Kim, H. Park, and S. Kim, "The growth and scintillation properties of $\text{Cs}_2\text{NaCeCl}_6$ single crystal," *J. Cryst. Growth*, vol. 311, pp. 2470–2473, 2009.
- [19] E. V. D. Van Loef, W. Mengesha, J. D. Valentine, P. Dorenbos, and C. W. E. van Eijk, "Non-proportionality and energy resolution of a $\text{LaCl}_3:10\%\text{Ce}^{3+}$ scintillation crystal," *IEEE Trans. Nucl. Sci.*, vol. 50, pp. 155–158, 2003.
- [20] W. E. van Eijk, J. T. M. de Haas, P. Dorenbos, K. W. K. W. Kramer, and H. U. Gudel, "Luminescence properties of Ce-doped $\text{Cs}_2\text{LiLaCl}_6$ crystals," in *Proc. 2005 IEEE NSS Conf. Rec.*, 2005, pp. 239–243.
- [21] J. Globo, W. H. Higgins, E. V. D. van Loef, and K. S. Shah, "Scintillation properties of 1 inch $\text{Cs}_2\text{LiYCl}_6:\text{Ce}$ crystal," *IEEE Trans. Nucl. Sci.*, vol. 55, pp. 1206–1209, 2008.
- [22] C. M. Combes, P. Dorenbos, C. W. E. van Eijk, K. W. Kramer, and H. U. Gudel, "Optical and scintillation properties of pure and Ce³⁺ doped $\text{Cs}_2\text{LiYCl}_6$ and $\text{Li}_3\text{YCl}_6:\text{Ce}^{3+}$ crystals," *J. Lumin.*, vol. 82, pp. 299–305, 1999.
- [23] K. S. Shah, J. Glodo, M. Klugerman, W. W. Moses, S. E. Derenzo, and M. J. Weber, "LaBr₃:Ce scintillators for gamma-ray spectroscopy," *IEEE Trans. Nucl. Sci.*, vol. 50, pp. 2410–2413, 2003.
- [24] P. Dorenbos, J. T. M. de Haas, and C. W. E. van Eijk, "Non-proportionality in the scintillation response and the energy resolution obtainable with scintillation crystals," *IEEE Trans. Nucl. Sci.*, vol. 42, pp. 2190–2202, 1995.
- [25] D. W. Aitken, B. L. Beron, G. Yenicyay, and H. R. Zulliger, "The fluorescent response of Na(Tl), CsI(Tl), CsI(Na), and $\text{CaF}_2(\text{Eu})$ to X-rays and low energy gamma rays," *IEEE Trans. Nucl. Sci.*, vol. 14, pp. 468–477, 1967.